are on these points, which are slightly different from one mode to another.

References

[1]Leissa, A. W., "On a Curve Veering Aberration," *Journal of Applied Mathematics and Physics (ZAMP)*, Vol. 25, No. 1, 1974, pp. 99–111.

[2]Kutter, J. R., and Sigillito, V. G., "On Curve Veering," *Journal of Sound and Vibration*, Vol. 75, No. 4, 1981, pp. 585–588.

[3]Triantafyllou, M. S., "Linear Dynamics of Cables and Chains," *Shock and Vibration Digest*, Vol. 16, No. 1, 1984, pp. 9–17.

[4]Schajer, G. S., "The Vibration of a Rotating Circular String Subject to a Fixed End Restraint," *Journal of Sound and Vibration*, Vol. 92, No. 1, 1984, pp. 11–19.

[5]Perkins, N. C., and Mote, C. D., Jr., "Comments on Curve Veering in Eigenvalue Problems," *Journal of Sound and Vibration*, Vol. 106, No. 3, 1986, pp. 451–463.

[6]Pierre, C., and Dowell, E. H., "Localization of Vibrations by Structural Irregularity," *Journal of Sound and Vibration*, Vol. 114, No. 3, 1987, pp. 547–564.

[7]Afolabi, D., "A Note on the Rouge Failure of Turbine Blades," *Journal of Sound and Vibration*, Vol. 122, No. 3, 1988, pp. 535–545.

[8]Pierre, C., "Mode Localization and Eigenvalue Loci Veering Phenomena in Disordered Structures," *Journal of Sound and Vibration*, Vol. 126, No. 3, 1988, pp. 485–502.

[9]Cornwell, P. J., and Bendiksen, O. O., "Localization of Vibrations in Large Space Reflectors," *AIAA Journal*, Vol. 27, No. 2, 1989, pp. 219–226.

[10]Happawana, G. S., Bajaj, A. K., and Nwokah, O. D. I., "A Singular Perturbation Analysis of Eigenvalue Veering and Modal Sensitivity in Perturbed Linear Periodic System," *Journal of Sound and Vibration*, Vol. 160, No. 2, 1993, pp. 225–242.

[11]Liu, X. L., "Derivation of Formulas for Perturbation Analysis with Modes of Close Eigenvalues," *Structural Engineering and Mechanics*, Vol. 10, No. 5, 2000, pp. 427–440.

A. Berman
Associate Editor

Genetic Algorithms for Optimization of Piezoelectric Actuator Locations

Lizeng Sheng* and Rakesh K. Kapania†
Virginia Polytechnic Institute and State University, Blacksburg, Virginia 24061-0203

Introduction

OPTIMAL placement of sensors/actuators has drawn significant attention recently due to its importance in many applications such as shape control, vibration control, acoustic control, buckling control, aeroelastic control, and health monitoring of structures. Various methods have been used to address this issue, including the method of placing piezoelectric actuators in the region of high average strain and away from areas of zero strain,[1] heuristic integer programming,[2] tabu search,[3] simulated annealing,[4] genetic algorithms,[5–7] etc.

Genetic algorithms (GAs) have attracted considerable attention due to their ability to solve large complex optimization problems. In this Note, two versions of GAs, GA version 1 and GA version 2, were used to solve two kinds of difficult, computationally intensive, combinatorial, and continuous large-scale optimization problems. The two problems are related to finding both a set of optimal locations and a set of corresponding optimal voltages for 30 piezoelectric actuators, from a maximum possible 193 candidate locations, with more than 1.28×10^{35} possible solutions, which will yield the best correction to the surface thermal distortions of a thin hexagonal spherical primary mirror (Fig. 1a) subjected to four different thermal distortions. In the first problem, a set of actuator locations was obtained for each of the four thermal distortions. In the second problem, only one set of actuator locations effective for all of the four thermal loads was determined. The latter is a more challenging, multicriterion optimization problem. A laminated triangular shell element[8] was used to model the mirror (Fig. 1b). The performance of the GAs and results of comparing with DeLorenzo's algorithm are presented.

GAs

GAs[9,10] are robust stochastic global optimization techniques based on the mechanism of natural selection and natural genetics. GAs were invented by Holland in the 1960s.[11] They are population-based search algorithms with selection, crossover, mutation, and inversion operations. The advantages and disadvantages of GAs were presented in Ref. 7.

In this study, two versions of GAs, GA version 1 and GA version 2, developed by the present authors from Carroll's FORTRAN GA driver,[12] have the following elements in common.

1) The encoding scheme is the same: the direct mapping, where the string would contain a 1 or 0 in the bits corresponding to the presence or absence of actuators.

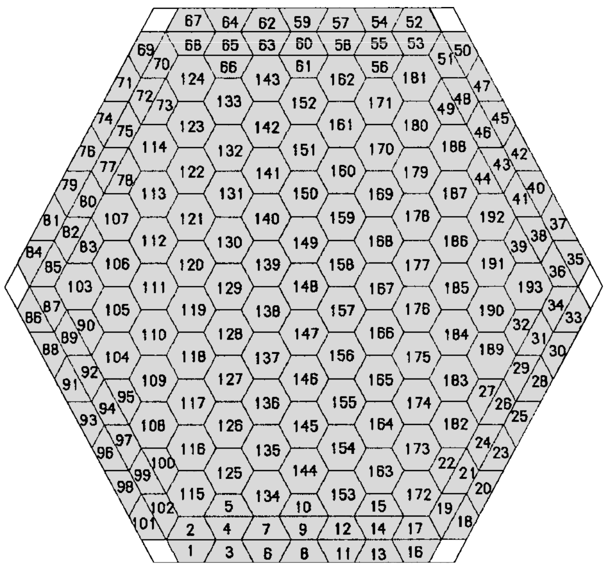

Fig. 1a Piezoelectric actuator candidate locations.

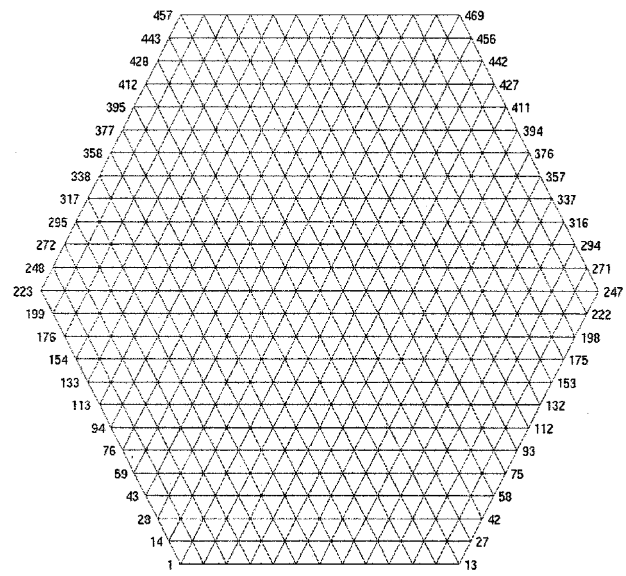

Fig. 1b Finite element mesh.

Received 28 Feburary 2000; presented as Paper 2000-1581 at the AIAA/ASME/ASCE/AHS/AHC 41st Structures, Structural Dynamics, and Materials Conference, Atlanta, GA, 3–6 April 2000; revision received 5 March 2001; accepted for publication 1 May 2001.

*Graduate Research Assistant, Department of Aerospace and Ocean Engineering. Student Member AIAA.

†Professor, Department of Aerospace and Ocean Engineering. Associate Fellow AIAA.

2) The selection scheme is the same: the tournament selection and elitism selection.

3) The crossover scheme is the same: uniform crossover with a rate of 0.5.

The main differences between versions 1 and 2 are as follows. First, the mechanism that preserves the best solution is different. In version 1, a randomly selected individual in the population is replaced by the best solution, but in version 2, the worst individual in the population is replaced by the best solution. Second, there are two important issues in the design of GAs: population diversity and selective pressure. Both of these are influenced by the size of the population. In version 1, the size of the population is fixed, but in version 2, the population size can vary during evolution.

Problem Definition

With 30 piezoelectric actuators, determine from a total of 193 candidate locations an optimal placement and corresponding optimal voltage for each actuator, to obtain the best correction to the surface thermal distortions of a thin hexagonal spherical primary mirror subjected to four different types of thermal loads (Fig. 1a). There are two kinds of optimization problems: One is to find a set of locations and corresponding voltages that get the best correction to the surface thermal distortions under each of the four types of thermal loads; the other is to find one set of locations and corresponding voltages that provide the best possible correction to the four surface thermal distortions caused by the four different thermal loads. Note that, for the second case, while the actuator locations are same for all four of the cases, the corresponding voltages may not be. The second problem is a multicriterion problem and obviously is a more challenging problem.

These are very large, difficult and computationally intensive combinatorial optimization problems. The number of different candidate sets is

$$^{193}C_{30} = \binom{193}{30} = \frac{193!}{30!(193-30)!} = 1.28866 \times 10^{35}$$

The geometry and material properties of the mirror and piezoelectric actuators are given in Table 4 in Ref. 2. The four types of temperature distributions at the lower surface of the mirror are given in Table 5 in Ref. 2.

Finite Element Modeling

A recently developed laminated triangular shell element[8] is used to model the mirror. The element is a combination of the discrete Kirchhoff theory (DKT) plate bending element and a membrane element derived from the linear strain triangular element with a total of 18 degrees of freedom (3 translations and 3 rotations per node). The piezoelectric strips are assumed to be perfectly bonded on the lower surface of the mirror and are modeled as a separate layer. The finite element model consists of 864 flat shell elements and 469 grid points (Fig. 1b). The mirror segment is assumed to be simple supported at the six vertices 1, 13, 223, 247, 457, and 469.

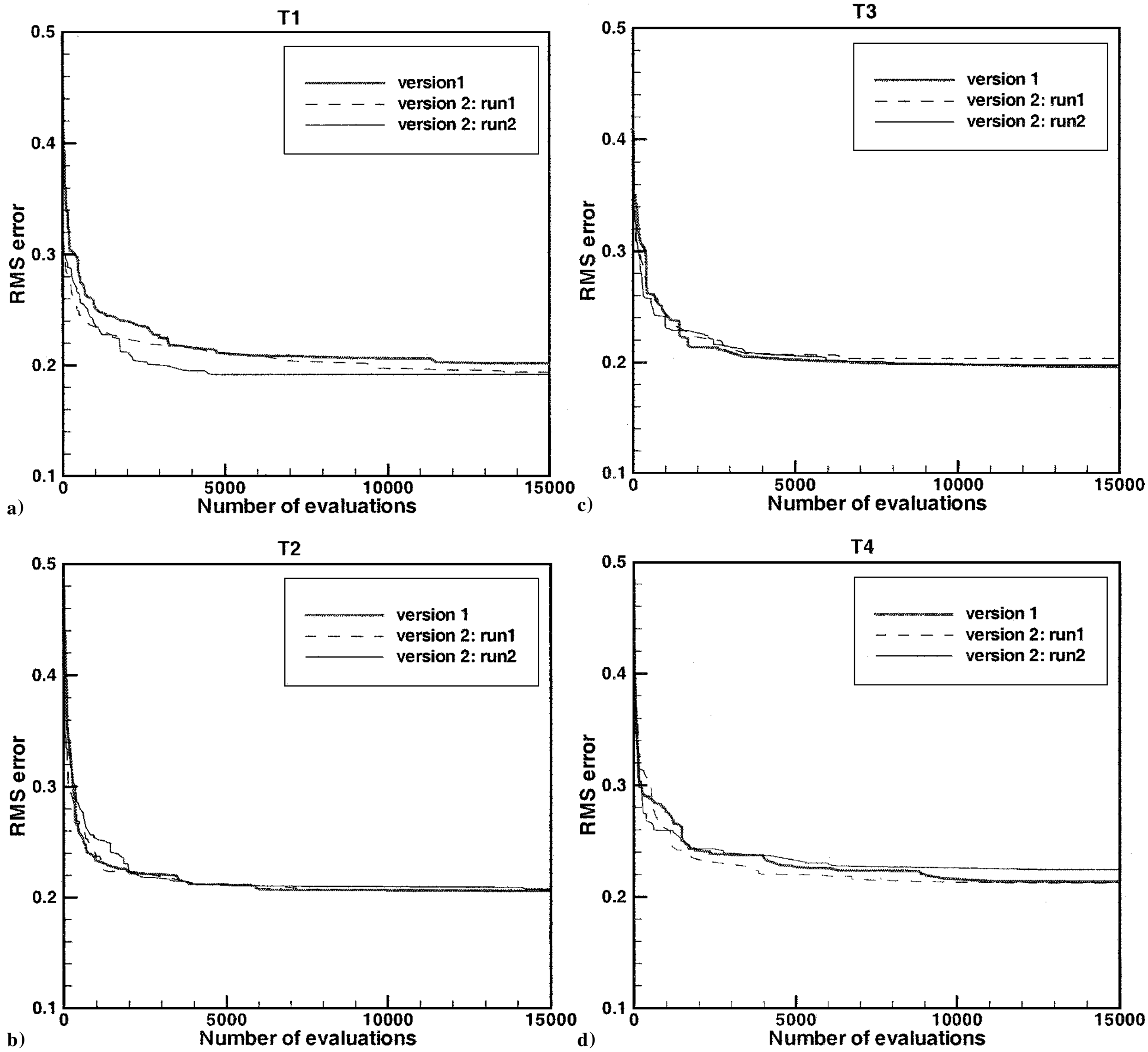

Fig. 2 Performance of the GAs vs the number of evaluations on a) thermal load T1, b) thermal load T2, c) thermal load T3, and d) thermal load T4.

Control Algorithms

The surface thermal distortions or the transverse displacements w of the mirror segment are corrected by applying the voltage across the thickness of the piezoelectric strip, which induces a distributed strain in the strip and, hence, in the mirror. The deformations considered are so small (of order of a few micrometers) that the correction u_i at any point can be assumed to be

$$u_i = \sum_{j=1}^{n} \alpha_{ij} V_j$$

where the control input V_j is the voltage applied across the jth piezoelectric strip and the influence coefficient α_{ij} is defined as the deformation caused at node i due to a unit voltage applied across the jth piezoelectric strip alone.

A matrix of influence coefficients of size $m \times n$ (where m is the total number of grid points in the finite element method model and n is the given number of piezoelectric actuators) is obtained from the finite element model by applying a unit voltage across each of the piezoelectric strips, one at a time. Given a type of thermal load T, a set of actuator locations L, and corresponding voltages V, a measure of the overall deviation or the rms error E is given by

$$E = E(T, L, V) = \sqrt{\frac{1}{m}\sum_{i=1}^{m}(w_i + u_i)^2}$$

$$= \sqrt{\frac{1}{m}\sum_{i=1}^{m}\left(w_i + \sum_{j=1}^{n}\alpha_{ij} V_j\right)^2}$$

To obtain the best correction, setting $\partial E/\partial V_k = 0$ gives

$$\sum_{i=1}^{m}\left(w_i + \sum_{j=1}^{n}\alpha_{ij} V_j\right)\alpha_{ij} = 0$$

that is, $[A]\{V\} = \{b\}$, where

$$A_{kj} = \sum_{i=1}^{m}\alpha_{ij}\alpha_{ik}, \qquad b_k = -\sum_{i=1}^{m} w_i \alpha_{ik}$$

For each set of locations, we can get the optimal voltages to minimize rms error. Different settings of actuator location have different optimal voltages and corresponding minimum rms error. Thus, the first optimization problem is to find a set of locations and corresponding voltages such that

$$E = \operatorname*{Min}_{L}\operatorname*{Min}_{V} E(T, L, V)$$

the second optimization problem is to find a set of locations and corresponding voltages such that

$$E = \operatorname*{Min}_{L}\operatorname*{Max}_{T}\operatorname*{Min}_{V} E(T, L, V)$$

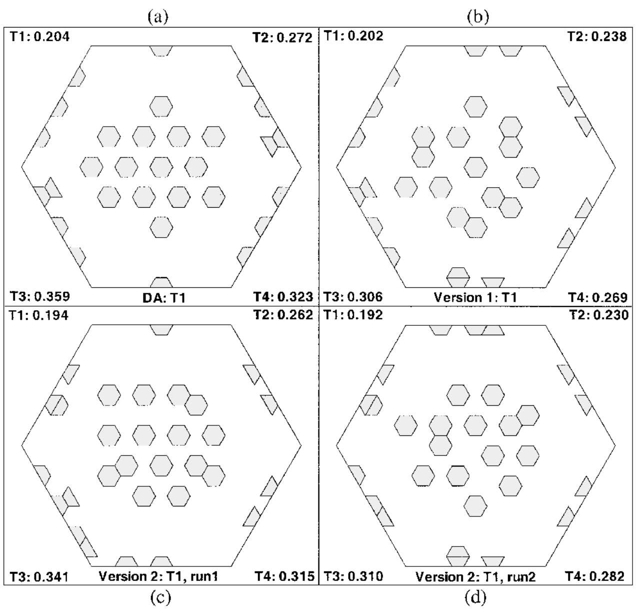

Fig. 3 Optimal location for the thermal load T1 obtained by a) the DeLorenzo algorithm, b) GA version 1, c) GA version 2, run1, and d) GA version 2, run2.

Results and Discussion

In this section, the results obtained by using the two versions of GAs to solve the two kinds of optimization problems are presented. To show the effectiveness of GAs, the corresponding results obtained by the DeLorenzo algorithm[2] are also presented.

The following parameters were used: version 1, population size 5, and restart control parameter diffrac = 0.06; version 2, run1, initial population size 10, population size 5, scale = 0.5, random = 0, and restart control parameter diffrac = 0.06; and version 2, run2, initial

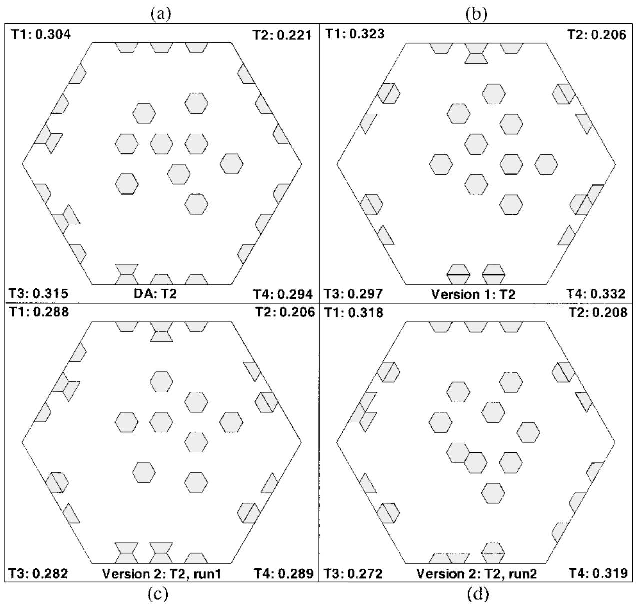

Fig. 4 Optimal location for the thermal load T2 obtained by a) the DeLorenzo algorithm; b) GA version 1; c) GA version 2, run1; and d) GA version 2, run2.

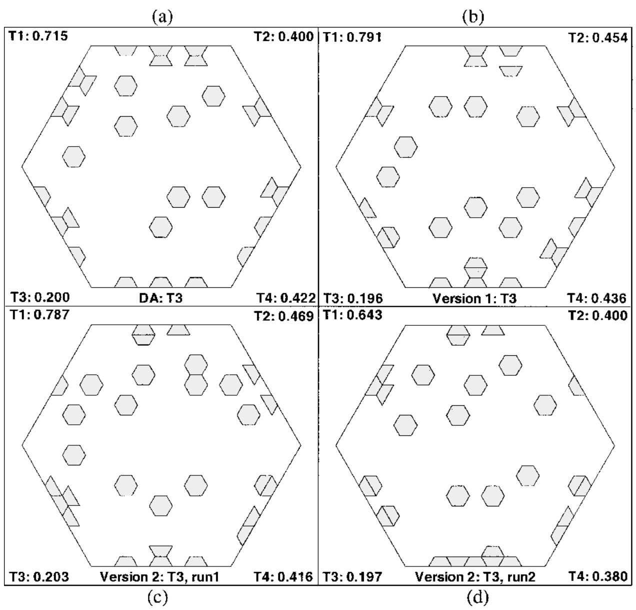

Fig. 5 Optimal location for the thermal load T3 obtained by a) the DeLorenzo algorithm; b) GA version 1; c) GA version 2, run1; and d) GA version 2, run2.

population size 10, population size 5, scale = 0.5, random = 0, and restart control parameter diffrac = 0.0.

Note that the new parameters initial population size, scale, and random were introduced in version 2. The parameter scale is used to adjust the selective pressure. The parameter random is used to control whether the initial population size and population size are randomly generated or not. When the parameter random equals 0, the initial population size and population size equal the preset values, respectively; otherwise, they equal the numbers generated randomly. The parameter diffrac is used to check the convergence of population. When this value is less than the preset value, the new populations are randomly generated.

The performance of the GAs on different types of thermal loads vs the number of evaluations is shown in Figs. 2a–2d. The number of evaluations for the case of 30 strips using the DeLorenzo algorithm is 18,256. Note that DA in Figs. 3–6 represents the results by using the DeLorenzo algorithm. Figure 7a also shows performance of the GAs for the second optimization problem. Results for optimal actuator locations for various cases of thermal loads considered are presented in Figs. 3–7. Note how the optimal locations, obtained to minimize a given type of thermal loads, perform for other types of thermal distortions. In general, it was seen that this performance of the actuators deteriorates (substantially, in some cases) when used for any other type of thermal loads. For example, the actuator location obtained to minimize distortions for the type 1 thermal load (Fig. 3a) is not as effective for reducing the other types of thermal distortions. When this set of actuator locations is used, the rms error for the type 1 distortions reduces to 0.204 (see top-left-hand corner in Fig. 3a), whereas the corresponding number is 0.272 for type 2 (top-right-hand corner in Fig. 3a), 0.359 for type 3 (bottom-left-hand corner in Fig. 3a), and 0.323 for type 4 (bottom-right-hand corner in Fig. 3a). Indeed, it was this deterioration in the performance of a given set of actuator locations for other types of thermal loads that led the present authors to seek one set of actuator locations that will give acceptable distortion reduction for all of the four types of thermal distortions (the second optimization problem). Figure 7 shows the one set of actuator locations that can be used for all of the four types of thermal distortions. The number of evaluations using genetic algorithms in this study is limited to 15,000.

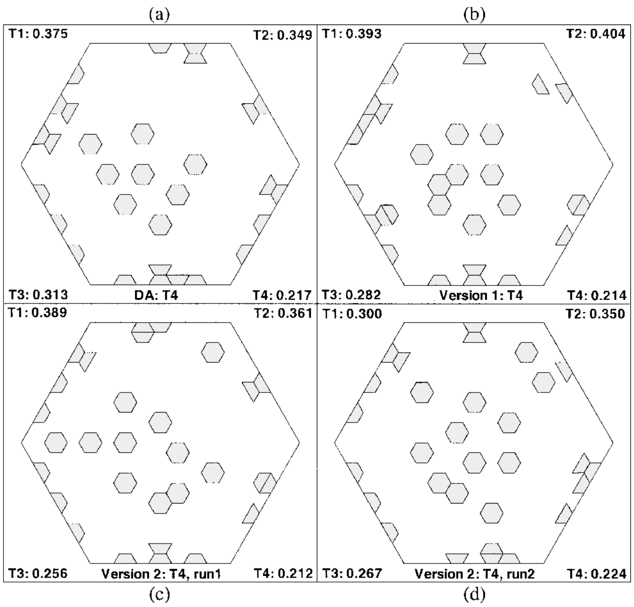

Fig. 6 Optimal location for the thermal load T4 obtained by a) the DeLorenzo algorithm; b) GA version 1; c) GA version 2, run1; and d) GA version 2, run2.

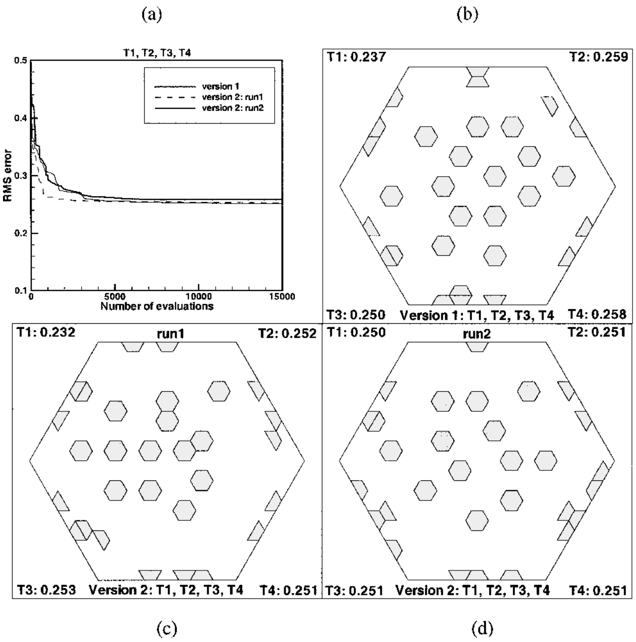

Fig. 7 Set of actuator locations: a) performance of the GAs vs the number of evaluations; b) optimal location for the thermal loads T1, T2, T3, and T4 obtained by GA version 1; c) GA version 2, run1; and d) GA version 2, run2.

The optimal voltages corresponding to optimal location under each type of thermal loads may be too high to generate in space. Several promising methods can be used to lower the control voltages.[7]

Conclusions

In this study, two versions of GAs (versions 1 and 2) have been developed to solve two kinds of combinatorial and continuous large-scale optimization problems of choosing 30 piezoelectric actuator locations from 193 candidate locations, with more than 1.28×10^{35} possible solutions, and optimal voltages in the design of a thin hexagonal spherical primary mirror to be used in the next generation of astronomical telescopes. One type of optimization problem is to find a set of locations and the corresponding voltages that gives us the best correction to the surface thermal distortions of the primary mirror under a given type of thermal loads; the other is to find one set of locations and corresponding voltages that provides the best correction to all of the surface thermal distortions caused by each of the four different thermal loads. Both types of problems are difficult and computationally intensive; the second one is a more challenging multicriterion optimization problem. The results show that both types of problems are multimodal optimization problems, that is, there is more than one optimal solution. This feature provides a great flexibility in the placement of piezoelectric actuators. The research reveals an important phenomenon in the application of GAs to a practical problem, namely, that the convergence to a solution may occur without reaching an optimal solution. This study shows that both of the GAs are robust in solving the described two kinds of optimization problems and can get modestly better results than the DeLorenzo algorithm and that the cost of the GAs is less than DeLorenzo's algorithm for the case of 30 actuators. Version 2 is more flexible, and, moreover, it got slightly better results than version 1 on the second kind of optimization problem. Considering so large complex search space with more than 1.28×10^{35} possible solutions, both of the GAs got better solutions within the limit of 15,000 evaluations. The research shows that both versions are effective in solving the two kinds of optimization problems of determining actuator locations for thermal distortion control.

Acknowledgments

The work was performed under a subcontract from University of Texas at Arlington, which is working under a grant from the National Science Foundation. We would like to thank Bernard Grossman, Department Head, Aerospace and Ocean Engineering, for providing considerable computational resources.

References

[1]Crawley, E. E., and de Luis, J., "Use of Piezoelectric Actuators as Elements of Intelligent Structures," *AIAA Journal*, Vol. 25, No. 10, 1987, pp. 1373–1385.

[2]Kapania, R. K., Mohan, P., and Jakubowski, A., "Control of Thermal Deformations of Spherical Mirror Segment," *Journal of Spacecraft and Rockets*, Vol. 35, No. 2, 1998, pp. 156-162; also AIAA Paper 96-4145, 1996.

[3]Padula, S. L., and Palumbo, D. L., "Optimal Sensor/Actuator Locations for Active Structural Acoustic Control," AIAA Paper 98-1865, 1998.

[4]Chen, G. S., Bruno, R. J., and Salama, M., "Optimal Placement of Active/Passive Members in Truss Structures Using Simulated Annealing," *AIAA Journal*, Vol. 29, No. 8, 1991, pp. 1327–1334.

[5]Rao, S. S., Pan, T. S., and Venkayya, V. B., "Optimal Placement of Actuators in Actively Controlled Structures Using Genetic Algorithms," *AIAA Journal*, Vol. 29, No. 6, 1991, pp. 942, 943.

[6]Furuya, H., and Haftka, R. T., "Combining Genetic and Deterministic Algorithms for Locating Actuators on Space Structures," *Journal of Spacecraft and Rockets*, Vol. 33, No. 3, 1996, pp. 422–427.

[7]Sheng, L., and Kapania, R. K., "Genetic Algorithms for the Optimization of Piezoelectric Actuator Locations," AIAA Paper 2000-1581, April 2000.

[8]Kapania, R. K., and Mohan, P., "Static, Free Vibration and Thermal Analysis of Composite Plates and Shells Using a Flat Triangular Shell Element," *Computational Mechanics: An International Journal*, Vol. 17, No. 5, 1996, pp. 343–357.

[9]Goldberg, D. E., *Genetic Algorithms in Search, Optimization, and Machine Learning*, Addison Wesley Longman, Reading, MA, 1989.

[10]Holland, J. H., "Genetic Algorithms," *Scientific American*, July 1992, pp. 66–72.

[11]Mitchell, M., *An Introduction to Genetic Algorithms*, MIT Press, Cambridge, MA, 1996.

[12]Carroll, D. L., FORTRAN Genetic Algorithm Driver, URL: http://www.aic.nrl.navy.mil:80/galist/src/#fortran.

E. Livne
Associate Editor

Simultaneous Qualitative Health Monitoring and Adaptive Piezoelectric Sensoriactuation

Jeffrey S. Vipperman*
University of Pittsburgh, Pittsburgh, Pennsylvania 15261

Introduction

THERE is currently a large effort underway to efficiently and economically detect damage in structures such as aircraft, machines, bridges, and buildings. Historically, inspections have been conducted manually, which has typically resulted in downtime, labor costs, and human oversight. Whereas some forms of structural damage are fairly obvious on inspection, other forms are not. This is particularly true of fiber-reinforced polymer composites, which have become increasingly popular in their use through the years. Diagnostic tools have been developed to facilitate damage detection and notification. Various detection techniques have employed ultrasound, x-ray radiation, electrostatics, electromagnetics, acoustic emission, thermal imaging, fiber optics, strain sensing, and modal- or eigenanalysis.

There are pros and cons to each of these methods. These techniques typically require skilled human interaction to interpret the results of diagnostic tests and make some judgment as to whether structural damage is present or not. In the least, expert systems[1] or neural networks[2,3] are developed/trained to add autonomy to the detection process. For both of these methods, healthy as well as damaged structures must be observed to develop the systems. In addition, many methods are not very suitable (x rays and thermal imaging[4]) to in situ operation due to the shear bulk of the equipment, as well as expense. These limitations are overcome for ultrasound analysis by using portable hand-held units, or by using surface-bonded or embedded piezoelectric patches for ultrasonic actuation and sensing.[5–7] One paper has reported an analytical examination using interdigital electrodes on piezoceramics for ultrasonic sources and receivers.[8] Single patches can be used in a pulse/echo manner, or one patch can send sound through the structure while another receives.[7] Common to all of these approaches is using very short wavelength ultrasound acoustic waves to measure the distance to a reflective impedance discontinuity, resulting from a structural boundary or internal damage. Analyzing large structures with this method can be tedious. In addition, certain types of damage are difficult to detect with ultrasound, such as surface delaminations, because they are adjacent the natural boundary of the structure.

Embedded optical fibers have also been used to detect damage in composite materials. In one study a fiber optic nervous system was created throughout a structure.[9] When damage occurs, the optical fibers will break, disrupting the travel of light and indicating damage. A two-dimensional grid of fibers can be used to locate certain types of damage to within the resolution of the fiber optic array. Methods of strain sensing using fiber optics have also been employed for damage detection in composite materials at the expense of increased complexity.[10]

A tremendous amount of work has been done using system response measurements. These techniques are based on the observation that the modal properties (resonant frequencies and damping) of a structure will change with damage.[11] Some form of modeling is required to quantify the natural characteristics of the structure before and after damage. Good examples of such are the mass and stiffness matrices from finite element models,[11,12] transfer function parameters,[13] or analysis of the structural impulse response.[6,14] Many of these methods are model based and can require great computational effort, for example, to solve an eigenvalue problem.[11] The use of piezoelectric transducers has served to simplify the hardware requirements of these techniques[7] as well as preclude mass or stiffness loading in nondestructive evaluation methods.[7,14] These transducers are also used for acoustic emission evaluation.[15] It is known that, when a structure fails, a series of high-frequency stress pulses (acoustic emission) occur that can be monitored by specialized hardware to detect the onset of failure.

The proposed method is most similar to the previously reported technique of electromechanical impedance monitoring.[16,17] This method involves performing ultrasonic (frequency-domain) measurements of the coupled electromechanical impedance of a piezoelement attached to a host structure,[18] followed by data processing, which determines a scaler damage parameter.

Whereas this method does implicitly identify the capacitance and loss factor of the piezoceramic element, there are some significant differences from the technique presented hereinafter. Namely, the proposed method operates in a much lower bandwidth (sonic vs ultrasonic), directly measures a single scaler damage-related parameter in the time domain, and, thus, is somewhat simpler to implement, and functions simultaneously and autonomously of the collocated self-sensing transducer that is used to implement the device. The low-frequency operation of the proposed technique tends to delocalize the damage detection behavior reported by the impedance method,[17] possibly making the techniques complementary.

An example of the qualitative structural health monitoring capabilities of the adaptive piezoelectric sensoriactuator (APSA) is presented. The APSA provides a collocated sensor/actuator pair from a single piezoceramic patch and has been experimentally demonstrated for various control applications[19,20] and for piezoelectric transducer health monitoring.[21] Qualitative structural health monitoring capabilities are demonstrated using real-time monitoring of the piezoelectric permittivity, which is already implicitly measured by the adaptive piezoelectric sensoriactuator. The method is relatively simple, cheap, and easy to apply to existing structures; requires little computational effort; and does not interfere with the transduction capabilities of the APSA when used for active structural control systems or other applications.

Received 23 February 1999; revision received 24 October 2000; accepted for publication 6 April 2001.

*Assistant Professor, Department of Mechanical Engineering, 648 Benedum Engineering Hall. Member AIAA.